New Insights Into Polymer Rheology in Porous Media

R.S. Seight, SPE, **Tianguang Fan,** SPE, and **Kathryn Wavrik,** SPE, New Mexico Petroleum Recovery Research Center; and **Rosangela de Carvalho Balaban,** SPE, Universidade Federal do Rio Grande do Norte

Summary

This paper clarifies the rheology of xanthan and partially hydrolyzed polyacrylamide (HPAM) solutions in porous media, especially at low velocities. Previous literature reported resistance factors (effective viscosities in porous media) and an apparent shear thinning at low fluxes that were noticeably greater than what is expected on the basis of viscosity measurements. The polymer component that causes the latter behavior is shown to propagate quite slowly and generally will not penetrate deep into a formation. Particularly for HPAM solutions, this behavior can be reduced or eliminated for solutions that experience mechanical degradation or flow through a few feet of porous rock. Under practical conditions where HPAM is used for enhanced oil recovery (EOR), the degree of shear thinning is slight or nonexistent, especially compared to the level of shear thickening that occurs at high fluxes.

Introduction

Polymer rheology in porous media affects both injectivity and sweep efficiency during a chemical-flooding-enhanced EOR process. At moderate-to-high fluid velocities in porous media, xanthan solutions show shear thinning that closely follows xanthan's viscosity behavior (Chauveteau 1982; Cannella et al. 1988; Hejri et al. 1991; Seight et al. 2009). However, at low velocities in short cores, the literature (Cannella et al. 1988; Hejri et al. 1991; Seight et al. 2009) reported that xanthan continues to show shear thinning, whereas viscosity data predict Newtonian behavior (the first Newtonian region of the Carreau model). Because most oil is displaced at low velocities, resolution of this discrepancy is needed for accurate representation of xanthan resistance factors when simulating chemical-flooding processes.

A related phenomenon occurs for HPAM solutions. In porous media, HPAM solutions have been well-documented to show shear thickening (also called dilatant, pseudodilatant, and viscoelastic behavior); the resistance factor increases with increased flux for moderate-to-high fluid velocities (Pye 1964; Smith 1970; Jennings et al. 1971; Hirasaki and Pope 1974; Seight 1983; Masuda et al. 1992; Seight et al. 2009). At low velocities in porous media, some authors reported a mild shear-thinning behavior (Heemskerk et al. 1984; Masuda et al. 1992; Delshad et al. 2008), while others report Newtonian or near-Newtonian behavior (Seight et al. 2009). As with xanthan, expectations based on viscosity measurements imply that Newtonian behavior should be observed at low velocities in porous media. Again, a need exists to resolve this discrepancy so that proper resistance factors can be used as input during estimation of oil recovery from EOR projects.

In this paper, we demonstrate how xanthan and HPAM rheology in porous media correlates with permeability and porosity. We confirm the existence of unexpectedly high resistance factors at low fluxes in short cores. We examine whether the polymer component that causes this behavior can propagate very far into a formation under practical conditions. Finally, we consider circumstances when shear thinning can be expected to materialize for HPAM solutions deep within a formation.

Xanthan

Resistance Factors Vs. Flux. For our first studies with xanthan, we used two Berea sandstone cores (55- and 269-md permeability) and one porous polyethylene core (5120-md permeability). The 55-md Berea sandstone core was 14.35 cm long with a square cross section of 11.34 cm^2. Porosity was 17%, and the pore volume (PV) was 27.7 cm^3. Two internal pressure taps divided the core into three sections with lengths of 2.2, 10.15, and 2 cm. The 269-md Berea sandstone core was 12.78 cm long, also with a square cross section of 11.34 cm^2. Porosity was 21.2%, and the PV was 30.8 cm^3. Two internal pressure taps divided the core into three sections with lengths of 2.39, 8.75, and 1.64 cm. The polyethylene core was 15.27 cm long with a square cross section of 11.64 cm^2. The PV was 62.8 cm^3. Two internal pressure taps divided the core into three sections with lengths of 2.54, 10.3, and 2.43 cm. Our previous research (Seight et al. 2006) demonstrated that the pore structure of porous polyethylene was quite similar to that for Berea sandstone, although the porosity was considerably higher (35% vs. 17% and 21.2% for the two Berea cores). The cores were initially saturated with 2.52%-total-dissolved-solids (TDS) brine (2.3% NaCl + 0.22% NaHCO$_3$). This brine was filtered through 0.45-μm filters and was used to prepare all polymer solutions. All experiments were performed at 25°C.

After saturation with brine, at least 20 PV of xanthan solution was injected to ensure that polymer retention was satisfied in the cores. The xanthan gum was supplied as a white powder by CP Kelco. This polymer had a molecular weight (MW) between 2 and 2.5 million Daltons and a pyruvate content of 4.5%. The injected polymer solution contained 0.06% (600 ppm) xanthan in brine. The low-shear-rate viscosity (i.e., the first Newtonian region) for this solution was 8 cp. After saturating the cores with this polymer solution, injection rates were varied over a wide range (from 0.0174 to 1,111 ft/D), and resistance factors were measured in the three sections of each core. **Fig. 1** plots resistance factors for the middle sections of the three cores.

Permeability Dependence of Rheology. Resistance factors can depend on permeability simply because the effective shear rate varies with pore size. A given rheological curve is expected to shift to higher velocities in proportion to the square root of the permeability ratio (Chauveteau 1982; Seight 1991). For our three cores, we found that resistance factor correlated quite well (see **Fig. 2**) using the parameter $u(1-\phi)/(\phi k)^{0.5}$, where u is flux (in ft/D), ϕ is porosity, and k is permeability (in md). With an original basis in a capillary-bundle model of porous media, this parameter (or a modification thereof) was used by many previous researchers (Hirasaki and Pope 1974; Chauveteau 1982; Durst et al. 1982; Duda et al. 1983; Heemskerk et al. 1984; Cannella et al. 1988; Wreath et al. 1990; Hejri et al. 1991; Seight 1991).

Consistent with previous literature (Cannella et al. 1988; Hejri et al. 1991), Fig. 2 confirms that xanthan solutions show shear-thinning or pseudoplastic behavior in porous media. The solid curve in Fig. 2 shows that the viscosity data parallels the resistance factor in the shear-thinning region. To make this match, shear rates (in s^{-1}, associated with the viscosity data) were divided by 310 when plotted on the x axis. (This value of 310 was strictly an empirical factor that was needed to make the shear-thinning portions of the curves match.)

Unexpectedly High Resistance Factors at Low Fluxes. Viscosities in this work were measured at 25°C using Anton Paar Physica
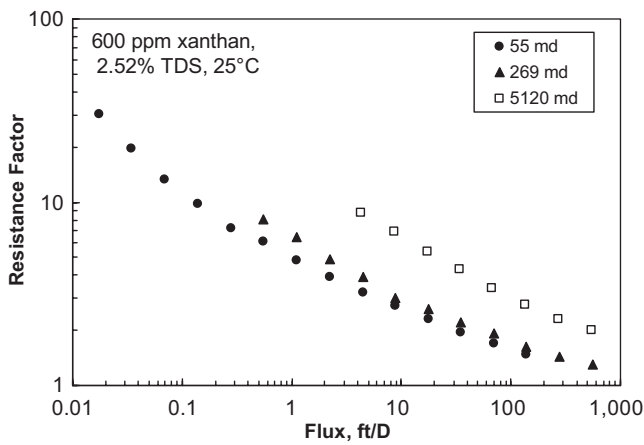
Fig. 1—Resistance factor vs. flux for 600 ppm xanthan.

Fig. 2—Correlated resistance factors for 600 ppm xanthan.

MCR 301 and Vilastic V-E rheometers at shear rates between 0.01 and 1,000 s^{-1}. For the xanthan solution, the viscosity at low shear rates exhibited a plateau value of 8 (i.e., 8 cp or a flow resistance 8 times greater than water; solid curve in Fig. 2). Consequently, on the basis of viscosity (vs. shear rate) data, we expected to see Newtonian (flow-rate-independent) behavior at low flux values. Instead, in 55-md Berea sandstone, resistance factors at low flux reached as high as 30 (solid circles in Fig. 2). This behavior was also reported for xanthan solutions by Cannella et al. (1988) and Hejri et al. (1991). In 269-md Berea and 5120-md porous polyethylene, we did not achieve sufficiently low velocities to observe this phenomenon (because of limitations in the accuracy of our pressure transducers at low pressure drops).

We were concerned that this apparent shear-thinning behavior in our short cores might be an experimental artifact (associated with microgels or very-high-MW polymer species) that could not be expected to propagate far into a real reservoir. To test this idea, we performed an experiment in a 57-md Berea sandstone core that was 122 cm long, with four equally spaced internal pressure taps, which created five 24.4-cm sections within the core. The core porosity was 17.3%, and the core cross section was 15.24 cm^2. The permeabilities of the five core sections were 53, 64, 65, 74, and 41 md, respectively, giving a composite permeability of 57 md. The core was saturated with filtered 2.52%-TDS brine (2.3% NaCl + 0.22% NaHCO$_3$), and our polymer solution contained 600-ppm CP Kelco xanthan in this same brine.

We injected 2.5 PV of xanthan solution at 5.17-ft/D flux. (One PV was 321 cm^3.) After this 2.5 PV, we varied the polymer-injection rate over a wide range (0.005–5 ft/D, using a total of 0.2 PV of additional injection). The resistance factor was measured at
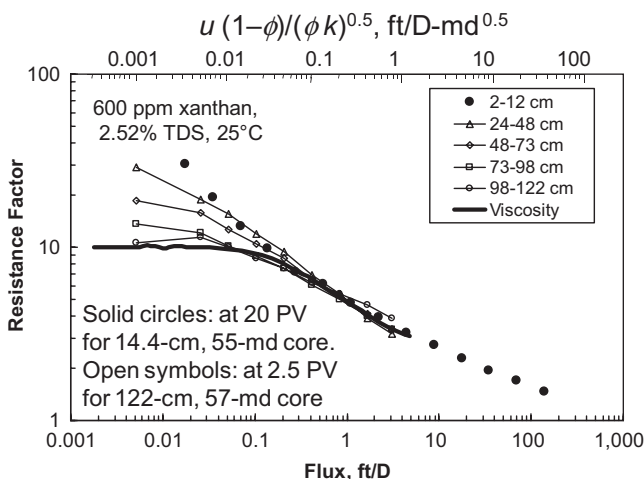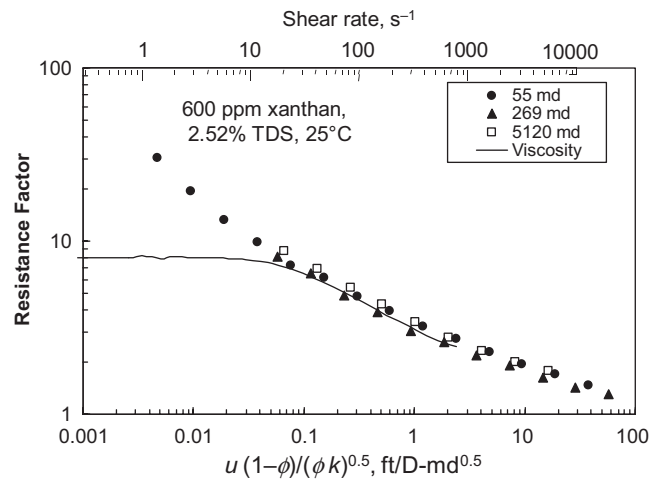
each rate in each of the five core sections. Values for the second through the fifth core sections are plotted in **Fig. 3**: open triangles for the second core section (24–48 cm from the core inlet), open diamonds for the third core section (48–73 cm), open squares for the fourth core section (73–98 cm), and open circles for the fifth core section (98–122 cm). (The first core section of this long core was treated as a filter.) Two other data sets are included for comparison in Fig 3. First, the solid circles plot resistance factors from the center 10.15-cm section of the short (14.35-cm) 55-md Berea core in Figs. 1 and 2 (with the data obtained after injecting 20 PV of xanthan solution). Second, the solid curve plots viscosity data (vs. adjusted shear rate) for the xanthan solution that was injected into the 122-cm core.

For flux values greater than 0.1 ft/D, the various data sets in Fig. 3 converged. However, they diverged as flux decreased below 0.1 ft/D. At the lowest fluxes, the resistance factors approached the zero-shear viscosity value as the distance progressed into the core. This result supports our original supposition that the unexpectedly high low-flux xanthan resistance factors may not practically propagate deep into a porous medium (i.e., a reservoir). Our presumption is that this phenomenon scales with core length and polymer throughput. If the core had been longer with the same volume injected, high resistance factors would not have reached as far from the core inlet. In contrast, if a greater polymer-solution volume had been injected into this same core, high resistance factors would have been seen throughout the core.

Calculations Quantifying Propagation of the High-Flow-Resistance Species. Calculations were performed to appreciate and quantify the degree to which the high low-flux xanthan resistance factors will propagate into 40- to 80-md sandstone. Injecting 2.5 PV of polymer solution into the 122-cm core translates to injecting 3.1 PV through to the fourth pressure tap, 4.2 PV through to the third tap, 6.2 PV through to the second tap, and 12.5 PV through to the first pressure tap. If a xanthan bank was injected into a horizontal well to reach 500 ft into the formation, the behavior seen in Core Section 5 of Fig. 3 (open circles, essentially the viscosity behavior) would occur out beyond 160 ft from the well [i.e., 500 ft/(2.5 PV)×(80% of the core length, associated with the beginning of the fifth core section)]. The behavior seen in Core Section 4 (open squares of Fig. 3) would occur from 120 to 160 ft from the well. The behavior seen in Core Section 3 (open diamonds of Fig. 3) would occur from 80 to 120 ft; and the behavior seen in Core Section 2 (open triangles of Fig. 3) would occur from 40 to 80 ft. Thus, depending on the level of the effect, the rate of propagation of the polymer species that causes the effect ranges from 1/6 (i.e., 80/500 ft) to 1/3 (i.e., 160/500 ft) the rate of propagation for the remainder of the polymer. These calculations are rudimentary and assume that only one population of microgels is present in the injected solutions. We recognize the possibility/probability

Fig. 3—Are high low-flux resistance factors able to propagate?

that a range of microgel sizes may exist, which may propagate at different rates.

For vertical wells, where flow is radial, the positions farthest from the wellbore and away from the most direct well-to-well streamlines would see the lowest flux values but would also experience the lowest polymer-throughput values. Consequently, the high xanthan resistance factors associated with the low-flux solid-circle data points in Figs. 2 and 3 are unlikely to materialize in these remote low-flux locations.

HPAM

After the xanthan experiments in the three cores mentioned in Figs. 1 and 2, we injected at least 19 PV of 0.25% (2,500 ppm) SNF Flopaam 3230S HPAM in 2.52%-TDS brine. (The manufacturer estimated the MW of this polymer at between 6 million and 8 million Daltons, with a degree of hydrolysis of 30%.) After saturation with this polymer, flux was varied over a wide range (0.035 to 135 ft/D) while measuring resistance factors. The results, expressed as resistance factor vs. the parameter $u(1-\phi)/(\phi k)^{0.5}$, are shown by the open symbols in **Fig. 4.**

Behavior at High Rates. Consistent with previous literature (Jennings et al. 1971; Durst et al. 1982; Southwick and Manke 1988; Seright et al. 2009), Fig. 4 confirms that HPAM resistance factors increase with increased flux at moderate-to-high flux values. This behavior was attributed to the viscoelastic character of HPAM and the elongational flow field in porous rock. In the past, this phenomenon has been called "shear thickening," "dilatant," "pseudodilatant," and "viscoelastic" behavior. For consistency, we will use the term "shear thickening," despite objections that might be raised by purists. Consistent with earlier work (Durst et al. 1982), the onset of the shear-thickening behavior correlated well with the parameter $u(1-\phi)/(\phi k)^{0.5}$. The solid curve in Fig. 4 shows viscosity data (again with shear rate divided by 310 plotted on the x axis). Interestingly, the onset of shear-thickening resistance factors in Fig. 4 correlated closely with the transition from Newtonian to shear-thinning viscosity behavior. This point will be discussed in detail later.

HPAM Shear-Thickening Behavior and Mechanical Degradation. HPAM solutions are susceptible to mechanical degradation (Maerker 1975, 1976; Seright 1983). The degree of mechanical degradation experienced by the polymer correlates with the applied pressure gradient (Seright 1983). This fact explains the differences in resistance factors at the highest velocities in Fig. 4. As the correlating parameter (x axis) increases above 0.4, resistance factor increased most steeply for the 5120-md data (open squares in Fig. 4) and least steeply for the 55-md data (open circles). For a given value of the correlating parameter in this region, pressure gradient varied inversely with the square root of permeability. Consequently, for a given value of the correlating parameter, as permeability decreased, pressure gradient increased, the level of polymer mechanical degradation increased, and the observed resistance factor decreased.

Behavior at Low Rates. For HPAM solutions, a viscosity plateau occurred at low shear rates (solid curve in Fig. 4), just as with xanthan solutions. Thus, we also expected resistance factors to approach a fixed value at low flux values. This expectation was met reasonably well by the low-flux HPAM resistance factors in 269-md Berea and 5120-md polyethylene. (Although, one might argue in favor of a very mild shear-thinning behavior in porous media.) However, in 55-md Berea, a significant shear-thinning behavior was noted at low flux (open circles in Fig. 4). We suspected that this behavior was caused by ultrahigh-MW polymers, or microgels (Chauveteau and Kohler 1984). These high-MW species may become mechanically entrapped (especially in less-permeable rock) and consequently reduce permeability and make the resistance factor appear significantly greater than the values expected from viscosity measurements. Important questions include these: Will this behavior occur deep within a reservoir, or is it simply a laboratory artifact associated with using relatively short cores? Can
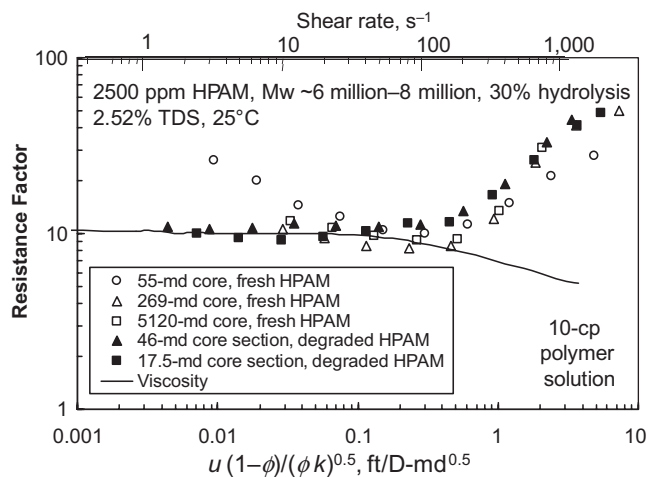

Fig. 4—Resistance factors for 2,500 ppm HPAM.

these high-MW species be expected to propagate very far into the porous rock of a reservoir? Will they be mechanically degraded into smaller species [as suggested by Seright et al. (1981)]? Will they be retained by the rock fairly close to the injection rock face [as suggested by Chauveteau and Kohler (1984)]?

HPAM Shear-Thinning Behavior and Mechanical Degradation. For the experiments reported to this point, the solutions were freshly prepared. In field applications, polymer solutions are likely to experience some level of mechanical degradation before penetrating deep into the reservoir. Most probably, the greatest level of mechanical degradation will occur as the polymer solutions first leave the wellbore and enter porous rock (Maerker 1975, 1976; Seright 1983, 2009). That is where the velocities are highest in the reservoir rock. Our previous experience suggested that the high-MW species are responsible for the HPAM causing permeability reductions and an unexpected shear thinning at low velocities in porous rock. These species are especially susceptible to mechanical degradation (Seright et al. 1981). To examine this issue further, we performed another set of experiments in which HPAM solutions were first forced through a core at a high pressure gradient. Specifically, we forced the polymer solutions through a 13.3-cm-long, 32-md Berea sandstone core using a pressure difference of 1,000 psi (2,292 psi/ft). This level of pressure gradient might be experienced by a polymer solution as it leaves an unfractured vertical wellbore to enter the formation rock.

The effluent from this core was reinjected into a second Berea core using a wide range of flux values to determine resistance vs. flux for the mechanically degraded polymer solutions. This process imitates what happens to a polymer solution as it flows radially away from a wellbore. The second core (13.9-cm total length, 38-md composite permeability) had three sections, with pressure taps located 2.2 cm from the inlet sandface and 1.9 cm from the outlet sandface. The second core section was 9.8 cm long and had a permeability of 46 md. The third core section (1.9 cm long) had a permeability of 17.5 md. [The first core section (2.2 cm long), with a permeability of 48 md, was treated as a filter for the core.]

The solid symbols in Fig. 4 plot resistance factor vs. flux for the second (46-md) core section (solid triangles) and for the third (17.5-md) core section (solid squares) for the degraded HPAM. As mentioned earlier, the open symbols in Fig. 4 plot resistance factors for undegraded (fresh) polymer solutions from 55-, 269-, and 5120-md cores. The onset of shear-thickening behavior occurred at approximately the same x-axis value for all five cases. At low flux values, resistance factors for four of the five curves leveled out (i.e., approached Newtonian behavior) at a value consistent with the viscosity of the polymer solution (10 cp). For the exception, fresh polymer injected into a 55-md core (open circles), resistance factors increased from 10 to 26 as flux decreased from 1.1 to 0.035 ft/D (i.e., the correlating parameter on the x axis decreased from
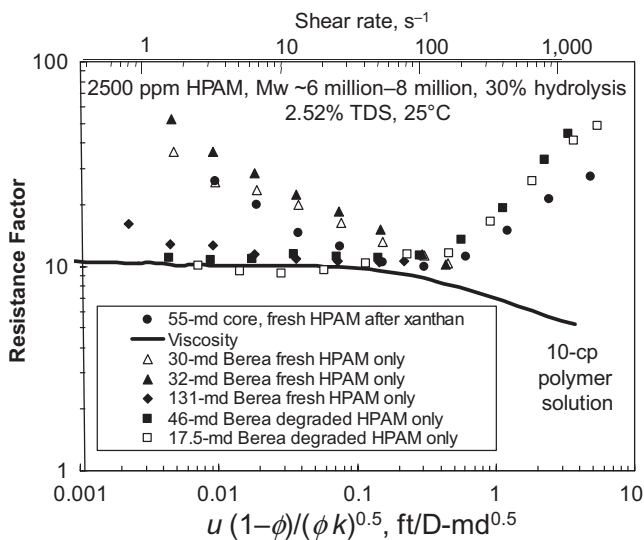
Fig. 5—HPAM resistance factors in new Berea sandstone cores.

Fig. 6—HPAM resistance factors in Berea sandstone after flow through a 122-cm core at low flux.

0.3 to 0.009 ft/D-md$^{0.5}$). When the experiment was repeated with mechanically degraded polymer in the 46- and 17.5-md Berea core segments (solid symbols in Fig. 4), Newtonian behavior was seen at low flux values. This result confirms that the mechanically degraded polymer did not contain the components that caused the apparent shear thinning in the 55-md core.

Viscosity vs. shear rate was measured for the polymer solution both before and after being forced through the first core. No significant viscosity difference was seen at any shear rate. These observations are consistent with earlier work (Seright et al. 1981) that revealed that the high-MW polymer species that cause high permeability reductions and high screen factors can be removed or degraded without causing large differences in viscosity behavior. For reservoir simulation and planning of field applications, there is considerable value in using laboratory data for polymers (especially HPAM) that were first forced through a core at a velocity characteristic of that seen near an injection well (Seright 1983; Sorbie 1991).

HPAM Flow After Xanthan. The reader may have noticed that we used the same three cores (55, 269, and 5120 md) for HPAM corefloods (Fig. 4) as during the previous xanthan corefloods (Figs. 1 and 2). One might wonder whether the unexpectedly high xanthan resistance factors in 55-md Berea sandstone at low flux in Fig. 2 were responsible for the subsequent behavior by HPAM in the same 55-md core in Fig. 4. To examine this possibility, several other experiments were performed in cores where only HPAM solutions were injected. In **Fig. 5,** the open and solid triangles show resistance-factor behavior during injection of fresh HPAM solution into two new 30- and 32-md Berea cores, respectively. These experiments show behavior very similar to that for the previously mentioned HPAM injection (after xanthan) in the 55-md core (solid circles replotted in Fig. 5) (i.e., the unexpected shear thinning still occurs at low fluxes). For comparison, we reproduced the experiments from Fig. 4 where mechanically degraded HPAM solutions were reinjected into 46- and 17.5-md Berea cores (squares in Fig. 5), and where Newtonian behavior was seen at low flux values.

Another experiment was performed where only HPAM solution was injected into a new 131-md Berea core (solid diamonds in Fig. 5). Note that, except for the lowest-rate data point, the low-flux resistance factors were reasonably close to the expectations based on viscosity measurements (solid curve in Fig. 5). These results suggest that the microgel species (that caused the unexpectedly high resistance factors and shear thinning at low fluxes in 30-, 32-, and 55-md cores) appeared to propagate reasonably well through 131-md Berea without causing unexpectedly high resistance factors.
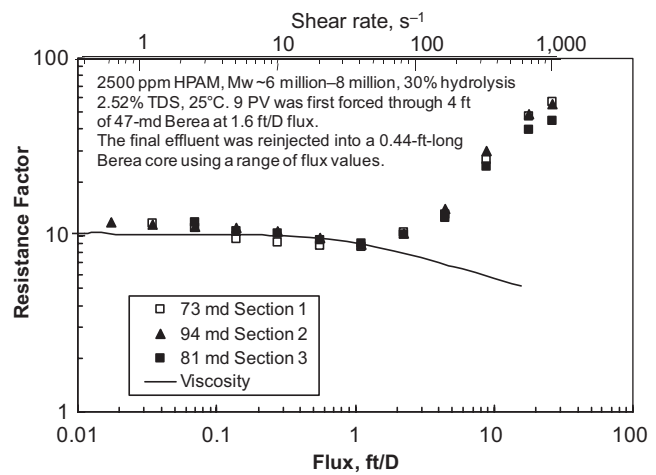
HPAM Behavior After Flow Through Rock at Low Flux. A previous experiment revealed that the species causing shear thinning in porous rock (associated with the open circles at low flux in Fig. 4) were removed or degraded when forced through rock at a high pressure gradient (2,292 psi/ft). We wondered whether it would also be removed by flow through rock at much lower pressure gradients. To address this question, a long Berea sandstone core was constructed, much like that used in Fig. 3. This core was 122 cm (4 ft) long and 15.24 cm^2 in cross section and had a PV of 321 cm^3, a porosity of 17.3%, and an average permeability of 47 md. We injected 9.2 PV of HPAM solution (2,500 ppm of SNF Flopaam 3230S in 2.52%-TDS brine) at a fixed flux of 1.6 ft/D. The effluent from the last part of this injection was then injected into a shorter Berea sandstone core, where we determined resistance factor vs. flux. The short core was 13.28 cm (0.44 ft) long and 11.34 cm^2 in cross section and had a PV of 26.3 cm^3. This core had two internal pressure taps, one located 2.12 cm from the inlet core face and the other at 1.88 cm from the outlet face. Consequently, the middle section of the core was 9.28 cm in length. The three sections of the core had permeabilities of 73, 94, and 81 md, respectively. **Fig. 6** plots resistance factor vs. flux for the three sections of this short core. In all core sections, near-Newtonian behavior was noted at low flux [i.e., the shear thinning observed at low flux for injection of fresh HPAM solution in a 55-md core (open circles of Fig. 4) was eliminated]. We attribute this effect (i.e., the shear thinning at low flux, associated with the open circles of Fig. 4) to a high-MW polymer species that is readily destroyed by mechanical degradation or retained by filtration. We do not anticipate that this species will propagate far into porous rock of a reservoir.

Permeability Dependence of Resistance Factors

As demonstrated in Figs. 2 and 4, polymer rheology in porous media correlated quite well using the parameter $u(1-\phi)/(\phi k)^{0.5}$. Beyond this rheological effect, polymers of a given type and MW are known to exhibit a permeability below which they experience difficulty in propagating through porous rock (Jennings et al. 1971; Vela et al. 1976; Zaitoun and Kohler 1987; Zhang and Seright 2007; Wang et al. 2008, 2009). As permeability decreases below this critical value, resistance factors, residual resistance factors, and polymer retention can increase dramatically. As recommended by Wang et al. (2008, 2009), the MW and size of the polymer should be chosen to be small enough so that the polymer will propagate effectively through all permeabilities and layers of interest—so this internal pore-plugging effect does not occur.

To investigate this effect further, we performed additional experiments using the 55-, 269-, and 5120-md cores that were mentioned earlier. In particular, after the experiments with SNF 3230S HPAM (open symbols in Fig. 4), we performed nearly identical experiments using a sequence of HPAM polymers with increasing

**TABLE 1—PERMEABILITY REDUCTION
AS A FUNCTION OF HPAM MW AND CORE PERMEABILITY**

Polymer	MW (million Daltons)	Ratio of Minimum F_r to Low-Shear-Rate Viscosity		
		55-md Core	269-md Core	5120-md Core
3230S (first)	6–8	1.0	0.9	1.0
3330S	8–19	1.4	1.3	1.1
3430S	10–12	1.2	1.2	1.2
3530S	15	1.7	1.9	1.6
3630S	18	2.6	2.1	1.4
3830S	18–20	4.5	1.7	1.8
6030S	20–22	6.3	2.3	1.5
3230S (last)	6–8	1.3	1.1	1.0

MW. The first column in **Table 1** lists the SNF Flopaam polymers in the sequence in which they were tested. The second column lists the polymer MWs, as estimated by the manufacturer. All polymers had 30% degree of hydrolysis, except 3830S and 6030S, which had 40% degree of hydrolysis. Details of the experimental results can be found in Seright (2009).

With one exception, the behavior of the various HPAM polymers was qualitatively similar to that for SNF 3230S. The exception was that a pore-plugging effect became increasingly evident as polymer MW increased and as core permeability decreased. This result can be seen in Table 1, after some explanation of the data listings. For each case in Table 1, the lowest resistance factor that was observed in the second (longest) core section (i.e., taken from the wide range of resistance-factor-vs.-flux measurements, such as those shown in Fig. 4) was divided by the polymer-solution viscosity associated with the first Newtonian region (e.g., the low-shear-rate plateau shown by the thick solid curve in Fig. 4). For the smallest polymer in Table 1 (3230S), this ratio was nearly unity in all three cores. As the polymer MW increased, this ratio increased, especially in the 55-md core. The ratio rose to 6.3 for the highest-MW polymer in the 55-md core. Because a high value for this ratio is an indicator of pore plugging, we expect the ratio to be less in more-permeable cores (e.g., 269 or 5120 md), for a polymer of given MW. Interestingly, when the lowest-MW polymer was subsequently injected, the ratio fell to 1.3, indicating that the pore-plugging effect was largely reversible in these cores. In less-permeable porous rock (17.5 and 46 md), we found the pore-plugging effect to be less reversible than observed in Table 1 (Seright 2009). These observations are qualitatively consistent with results reported by previous researchers (Jennings et al. 1971; Vela et al. 1976; Wang et al. 2008). The partial reversibility of the plugging effect could be attributed to hydrodynamic polymer retention (Maerker 1973; Chauveteau 1981).

Can HPAM Solutions Show Shear Thinning in Porous Media Deep Within a Formation?

Along with others, Chauveteau (1981) noted that HPAM solutions showed shear-thickening behavior at moderate to high velocities in porous media. However, he speculated that, at moderate to low flux values in capillary constrictions or in porous media, HPAM resistance factors might show shear-thinning behavior and, ultimately, show Newtonian behavior at the very lowest velocities. Consequently, he suggested that resistance factors should exhibit a minimum value at intermediate fluxes. Data published by Heemskerk et al. (1984), Masuda et al. (1992), and Delshad et al. (2008) could be viewed as indicating that HPAM in porous media exhibits a subtle shear thinning at low fluxes and a shallow minimum in resistance factor at intermediate fluxes. The open squares in Fig. 6 may support this view for freshly prepared 900-ppm HPAM (SNF Flopaam 3830S) in 2.52%-TDS brine when flowing through 5120-md porous polyethylene. However, the degree of shear thinning that was reported or observed was slight, and the existence of the shallow minimum is debatable. An earlier publication (Seright

et al. 2009) proposed that the observed shear thinning for HPAM solutions at low flux values in porous media could be an experimental artifact because of (1) the use of insufficiently accurate pressure transducers, (2) inadequate temperature control, and (3) a polymer MW that is too high to propagate without forming an internal or external filter cake (i.e., if the polymer contains significant concentrations of microgels or high-MW species that are too large to flow efficiently through the pore structure). The latter point was demonstrated earlier in this paper. Introduction of air into the core can also induce apparent shear thinning. If these experimental artifacts are avoided, can shear thinning occur during flow of polymer solutions in cores?

HPAM in Very-Low-Salinity Water. The work reported to this point was performed in brines with moderate-to-high salinity (at least 0.3% TDS). Gogarty (1967) reported a definitive shear thinning in cores for water containing 1,200 to 1,800 ppm of HPAM with less than 700 ppm (0.07%) TDS. Thus, it appears that shear thinning could materialize for HPAM solutions in porous rock if the salinity is sufficiently low. To confirm this possibility, we prepared HPAM solutions in distilled water and injected them at various rates into a 5120-md porous polyethylene core. **Fig. 7** shows the results using SNF Flopaam 3830S HPAM (with MW from 18 million to 20 million Daltons and degree of hydrolysis of 40%). For 400 ppm HPAM in distilled water (solid diamonds in Fig. 7), shear-thinning behavior was noted for flux values between 0.06 and 4.3 ft/D. The slope was −0.56 for a plot of ln(resistance factor) vs. ln(flux). A similar slope was noted for 1,000 ppm HPAM in distilled water for flux values between 0.135 and 4.3 ft/D (solid squares in Fig. 7). However, for higher flux values, the resistance factors leveled off and began a gradual increase. This latter behavior
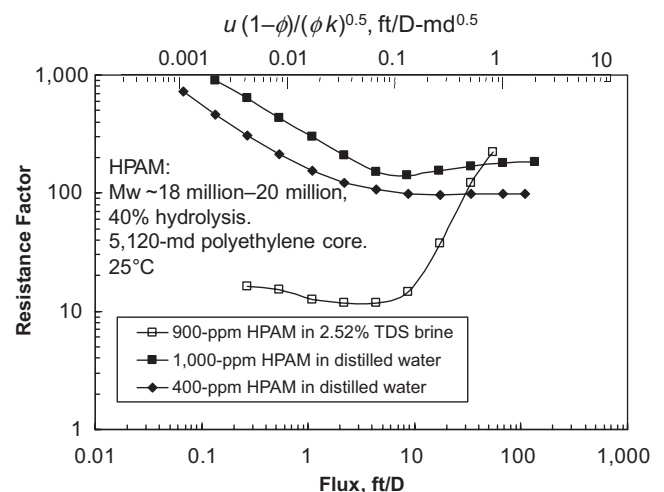

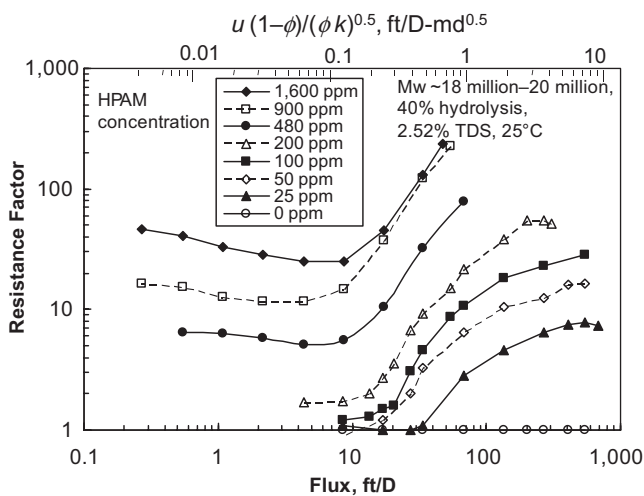Fig. 7—Shear thinning by HPAM solutions in porous media.

Fig. 8—Onset of shear thickening vs. HPAM concentration in a 5120-md core.

may be because of the viscoelastic nature of the polymer. Interestingly, the slope of plots of ln(viscosity) vs. ln(shear rate) were −0.85 for 400 ppm HPAM and −0.94 for 1,000 ppm HPAM. Thus, the very strong shear-thinning character of these solutions was moderated considerably during flow through porous media.

As mentioned earlier, the open squares in Fig. 7 show the behavior of 900 ppm HPAM in 2.52%-TDS brine. Consistent with Fig. 4, this curve shows a strong shear-thickening behavior at moderate-to-high flux values and near-Newtonian behavior at low flux values. (Although one could argue for the existence of a shallow minimum between 1 and 7 ft/D.) Thus, two key points may be taken from Fig. 7, along with our other results. First, HPAM solutions can show a definitive shear-thinning behavior at low flux values in porous media if the solvent is distilled water (or a solvent with very low salinity). Second, for HPAM solutions in more practical brines (i.e., > 0.3% TDS), Newtonian or near-Newtonian behavior is expected at low flux values far into a reservoir.

In Fig. 7, why is the character of the HPAM curves for distilled water (solid symbols) so different from that of HPAM in brine (open squares)? In saline brine, HPAM molecules exist as a coiled ball. A substantial amount of energy must be expended to uncoil this HPAM ball so the polymer molecules can flow through pore constrictions. That explains the dramatic shear-thickening seen at moderate-to-high fluxes (open squares in Fig. 7). For HPAM in distilled water, the polymer molecules are already highly expanded because of the unshielded electrostatic repulsion between anionic groups along the polymer chains. Consequently, very little energy is needed to stretch the polymer molecules into a configuration that can readily flow through pore throats. That explains why little or no shear thickening is seen at moderate-to-high flux in distilled water.

Relation Between the Onset of Shear Thinning in a Viscometer Vs. the Onset of Shear Thickening in Porous Media. As shear rate is increased for a polymer solution in a viscometer, a shear rate is encountered that marks the transition from Newtonian behavior to shear thinning. This transition shear rate is associated with the "longest relaxation time in the linear viscoelastic spectrum" (Graessley 1974). Some think of this point as the shear rate at which polymer conformations experience their first departure from a random coil configuration. The onset of shear thickening by HPAM solutions in porous media is also associated with a change in polymer conformation—specifically, where the polymers undergo a coil-stretch transition, resulting in highly extended polymer conformations and large extensional stresses (Durst et al. 1982; Southwick and Manke 1988). A comparison of the solid curve and the data points in Fig. 4 implies that these two transition points (i.e., the transition from Newtonian behavior to shear thinning in a viscometer and the onset of shear thickening in

porous media) might coincide. To explore this idea, we performed experiments using various concentrations (25 to 1,600 ppm) of SNF Flopaam 3830S in 2.52%-TDS brine. For this polymer under these conditions, we determined C^* (the concentration at which polymer behavior transitions from dilute to semidilute behavior) to be 200 ppm.

Fig. 8 plots resistance factor vs. flux during injection of many polymer solutions into a 5120-md porous polyethylene core. For polymer concentrations even as low as 25 ppm (one-eighth the value of C^*), shear thickening was evident. In contrast, viscosity vs. shear rate showed Newtonian behavior, with a value very close to 1 cp. As described in the literature (Durst et al. 1982), the elongational flow field associated with porous media can accentuate viscoelastic behavior that is not apparent from a pure shear field. This observation provides our first reason to doubt that the transition from Newtonian behavior to shear-thinning behavior in a viscometer correlates directly with the onset of shear thickening in porous media.

In Fig. 8, as polymer concentration increased from C^* (200 ppm) to 1,600 ppm, the onset of shear thickening decreased by a factor of two. For comparison, from viscosity-vs.-shear-rate data, the shear rate at the transition from Newtonian behavior to shear thinning decreased by a factor of 10 (from 10 to 1 s⁻¹) over the same range of polymer concentrations. Because the variation in transition-from-Newtonian-to-shear-thinning shear rate (10, from the viscosity data) was much greater than the variation in onset of shear thickening (2, from resistance-factor data), the apparent correlation between the two transitions seen in Fig. 4 must be coincidental.

At low flux values in Fig. 8, the curves for the three highest polymer concentrations show slight shear thinning. The slopes of these curves were −0.236 for 1,600 ppm HPAM and −0.114 for 480 ppm HPAM. For comparison, the slopes of the shear-thinning portions of ln(viscosity)-vs.-ln(shear rate) curves were −0.218 and −0.127 for the two concentrations, respectively. The similarity of the shear-thinning slopes from viscosity and core data suggests that shear thinning might occur in porous media, even in saline brines. This information also indicates that the apparent correlation between the two transitions seen in Fig. 4 was coincidental.

The Depletion-Layer Concept. Most of this paper has focused on observations where the resistance factor appears the same as or greater than that expected from viscosity measurements. Some literature reports suggest that the apparent viscosity in porous media is actually less than low-shear viscosities that are measured in a viscometer (Chauveteau 1981; Sorbie 1991). These observations were attributed to a depletion layer, which developed because the center of mass for a large polymer molecule was sterically unable to approach within a certain distance from pore walls. If a layer of low-viscosity water coats pore walls, this layer presumably could lubricate flow for the more-viscous polymer solution that exists farther away from the walls. Consequently, the apparent viscosity in porous media might appear less than the polymer-solution viscosity measured in a viscometer.

Although excluded-volume effects are well-accepted in polymer chromatography, the preceding arguments are not without controversy in the petroleum literature because of the way that the apparent polymer viscosity in porous media was determined. In our work, we simply report the resistance factor (i.e., the brine mobility before polymer injection divided by the polymer-solution mobility). This is a well-defined parameter that derives directly from the Darcy equation and measurements of pressure drops and flow rates. Advocates of the depletion-layer effects use a different method to determine apparent polymer viscosity in porous media. Specifically, they flush water through the core after polymer injection to determine the permeability reduction or residual resistance factor. The resistance factor during polymer injection is then divided by the residual resistance factor to determine the apparent polymer viscosity in porous media. Unfortunately, several experimental factors can lead to incorrect measurement of high residual resistance factors, which, in turn, lead to calculation of unexpectedly low apparent polymer viscosities in porous media.

These factors could include insufficient brine flushed through the core before recording the brine mobility, face plugging during brine injection, air injection, or any other factor that causes an excess pressure drop during measurement of post-polymer brine mobility. Although we recognize the existence and importance of inaccessible pore volume and depletion-layer effects during polymer flow through porous media, we advise caution when back calculating apparent polymer viscosities in porous media using residual resistance factors.

Significance of Observations. For HPAM solutions with a sufficiently low salinity or sufficiently high polymer concentration, shear thinning can be observed in porous media at moderate to low fluxes. However, the degree of shear thinning was slight, especially compared to the level of shear thickening at higher fluxes.

The work in this paper indicates that, under practical conditions for chemical-flooding field applications, HPAM solutions show Newtonian or near-Newtonian behavior at low flux values, if ultrahigh-MW polymer species are not present. Why is this point worth arguing? The reason is that cases exist where experimental artifacts and/or ultrahigh-MW polymer species suggest that strong shear thinning occurs at low velocities in short corefloods. If this behavior is assumed to translate directly to a reservoir scale, it leads to (1) an overly complex representation of polymer resistance factors and (2) prediction of resistance factors that are too high far into a formation. Also, most chemical-flooding simulators have incorrectly assumed that the shear-thinning behavior observed in HPAM solutions in a viscometer will be directly applicable in porous rock, ignoring the importance of shear thickening at higher velocities. This incorrect assumption leads to (1) an overly optimistic prediction of polymer injectivity if wells are not fractured and (2) often an incorrect prediction that fractures will not be open during polymer injection.

Conclusions

- At low velocities in short cores with sufficiently low permeability (e.g., 55 md), fresh xanthan solutions show shear thinning whereas viscosity data predict Newtonian behavior (the first Newtonian region of the Carreau model). If the polymer component that causes this behavior is removed by flowing the polymer solutions through a few feet of rock, resistance-factor-vs.-flux data closely follow expectations from viscosity-vs.-shear-rate data. The polymer component that caused the unexpected shear thinning at low fluxes propagates through 40- to 80-md Berea at one-sixth to one-third the rate for the remainder of the xanthan solution.
- In short cores with sufficiently low permeability (e.g., 55 md), shear thinning can be observed for fresh HPAM solutions at low fluxes that is much greater than the effect anticipated from viscosity-vs.-shear-rate data. However, this shear thinning may be substantially reduced or eliminated either by exposing the solution to high flux (i.e., characteristic of that seen near an unfractured injection well) or by passing the solution through a few feet of rock at low flux. We attribute this effect to a high-MW polymer species that is readily destroyed by mechanical degradation or retained by filtration. We do not anticipate that this species will propagate far into porous rock of a reservoir.
- For HPAM solutions with a sufficiently low salinity or sufficiently high polymer concentration, shear thinning can be observed in porous media at moderate-to-low fluxes. However, under practical conditions where HPAM is used for EOR, the degree of shear thinning is slight or nonexistent, especially compared to the level of shear thickening that occurs at high fluxes.

Nomenclature

C^* = critical polymer overlap concentration, ppm
F_r = resistance factor (water mobility/polymer-solution mobility)
k = permeability, darcies [μm^2]
u = flux, ft/D [m/d]
μ = viscosity, cp [mPa·s]
ϕ = porosity

References

Cannella, W.J., Huh, C., and Seright, R.S. 1988. Prediction of Xanthan Rheology in Porous Media. Paper SPE 18089 presented at the SPE Annual Technical Conference and Exhibition, Houston, 2–5 October. doi: 10.2118/18089-MS.

Chauveteau, G. 1981. Molecular Interpretation of Several Different Properties of Flow of Coiled Polymer Solutions Through Porous Media in Oil Recovery Conditions. Paper SPE 10060 presented at the SPE Annual Technical Conference and Exhibition, San Antonio, Texas, USA, 4–7 October. doi: 10.2118/10060-MS.

Chauveteau, G. 1982. Rodlike Polymer Solutions Flow Through Fine Pores: Influence of Pore Size on Rheological Behavior. *Journal of Rheology* **26** (2): 111–142. doi: 10.1122/1.549660.

Chauveteau, G. and Kohler, N. 1984. Influence of Microgels in Polysaccharide Solutions on Their Flow Behavior Through Porous Media. *SPE J.* **24** (3): 361–368; *Trans.*, AIME, **277**. SPE-9295-PA. doi: 10.2118/9295-PA.

Delshad, M., Kim, D.H., Magbagbeolz, O.A., Huh, C., Pope, G.A., and Tarahhom, F. 2008. Mechanistic Interpretation and Utilization of Viscoelastic Behavior of Polymer Solutions for Improved Polymer-Flood Efficiency. Paper SPE 113620 presented at the SPE/DOE Symposium on Improved Oil Recovery, Tulsa, 19–23 April. doi: 10.2118/113620-MS.

Duda, J.L., Hong, S.A., and Klause, E.E. 1983. Flow of Polymer Solutions in Porous Media: Inadequacy of the Capillary Model. *Ind. Eng. Chem. Fund.* **22** (3): 299–305. doi: 10.1021/i100011a005.

Durst, F., Haas, R., and Interthal, W. 1982. Laminar and Turbulent Flows of Dilute Polymer Solutions: A Physical Model. *Rheologica Acta* **21** (4–5): 572–577. doi: 10.1007/BF01534350.

Gogarty, W.B. 1967. Mobility Control with Polymer Solutions. *SPE J.* **7** (2): 161–173. SPE-1566-PA. doi: 10.2118/1566-PA.

Graessley, W.W. 1974. The Entanglement Concept in Polymer Rheology. *Adv. Polymer Sci.* **16** (1): 126.

Heemskerk, J., Rosmalen, R.J., Janssen-van, R., Hotslag, R.J., and Teeuw, D. 1984. Quantification of Viscoelastic Effects of Polyacrylamide Solutions. Paper SPE 12652 presented at the SPE/DOE Enhanced Oil Recovery Symposium, Tulsa, 15–18 April. doi: 10.2118/12652-MS.

Hejri, S., Willhite, G.P., and Green, D.W. 1991. Development of Correlations to Predict Biopolymer Mobility in Porous Media. *SPE Res Eng* **6** (1): 91–98. SPE-17396-PA. doi: 10.2118/17396-PA.

Hirasaki, G.J. and Pope, G.A. 1974. Analysis of Factors Influencing Mobility and Adsorption in the Flow of Polymer Solution Through Porous Media. *SPE J.* **14** (4): 337–346. SPE-4026-PA. doi: 10.2118/4026-PA.

Jennings, R.R., Rogers, J.H., and West, T.J. 1971. Factors Influencing Mobility Control by Polymer Solutions. *J Pet Technol* 23 (3): 391–401; *Trans.*, AIME, **251**. SPE-2867-PA. doi: 10.2118/2867-PA.

Maerker, J.M. 1973. Dependence of Polymer Retention on Flow Rate. *J Pet Technol* **25** (11): 1307–1308. SPE-4423-PA. doi: 10.2118/4423-PA.

Maerker, J.M. 1975. Shear Degradation of Partially Hydrolyzed Polyacrylamide Solutions. *SPE J.* **15** (4): 311–322; *Trans.*, AIME, **259**. SPE-5101-PA. doi: 10.2118/5101-PA.

Maerker, J.M. 1976. Mechanical Degradation of Partially Hydrolyzed Polyacrylamide Solutions in Unconsolidated Porous Media. *SPE J.* **16** (4): 172–174. SPE-5672-PA. doi: 10.2118/5672-PA.

Masuda, Y., Tang, K.-C., Mlyazawa, M., and Tanaka, S. 1992. 1D Simulation of Polymer Flooding Including the Viscoelastic Effect of Polymer Solution. *SPE Res Eng* **7** (2): 247–252. SPE-19499-PA. doi: 10.2118/19499-PA.

Pye, D.J. 1964. Improved Secondary Recovery by Control of Water Mobility. *J Pet Technol* **16** (8): 911–916; *Trans.*, AIME, **231**. SPE-845-PA. doi: 10.2118/845-PA.

Seright, R.S. 1983. The Effects of Mechanical Degradation and Viscoelastic Behavior on Injectivity of Polyacrylamide Solutions. *SPE J.* **23** (3): 475–485. SPE-9297-PA. doi: 10.2118/9297-PA.

Seright, R.S. 1991. Effect of Rheology on Gel Placement. *SPE Res Eng* **6** (2): 212–218; *Trans.,* AIME, **291.** SPE-18502-PA. doi: 10.2118/18502-PA.

Seright, R.S. 2009. Use of Polymers to Recover Viscous Oil from Unconventional Reservoirs. First Annual Report, U.S. Department of Energy, DOE Contract No.: DE-NT0006555, US DOE, Washington, DC (October 2009).

Seright, R.S., Maerker, J.M., and Holzwarth G. 1981. Mechanical Degradation of Polyacrylamides Induced by Flow Through Porous Media. *American Chemical Society Polymer Preprints* **22** (August): 30–33.

Seright, R.S., Prodanovic, M., and Lindquist, W.B. 2006. X-Ray Computed Microtomography Studies of Fluid Partitioning in Drainage and Imbibition Before and After Gel Placement. *SPE J.* **11** (2): 159–170. SPE-89393-PA. doi: 10.2118/89393-PA.

Seright, R.S., Seheult, M., Kelco, C.P., and Talashek, T. 2009. Injectivity Characteristics of EOR Polymers. *SPE Res Eval & Eng* **12** (5): 783–792. SPE-115142-PA. doi: 10.2118/115142-PA.

Smith, F.W. 1970. The Behavior of Partially Hydrolyzed Polyacrylamide Solutions in Porous Media. *J Pet Technol* **22** (2): 148–156. SPE-2422-PA. doi: 10.2118/2422-PA.

Sorbie, K.S. 1991. *Polymer-Improved Oil Recovery*, 115, 206, 207. Glasgow, Scotland: Blackie & Sons.

Southwick, J.G. and Manke, C.W. 1988. Molecular Degradation, Injectivity, and Elastic Properties of Polymer Solutions. *SPE Res Eng* **3** (4): 1193–1201. SPE-15652-PA. doi: 10.2118/15652-PA.

Vela, S., Peaceman, D.W., and Sandvik, E.I. 1976. Evaluation of Polymer Flooding in a Layered Reservoir with Crossflow, Retention, and Degradation. *SPE J.* **16** (2): 82–96. SPE-5102-PA. doi: 10.2118/5102-PA.

Wang, D.M., Dong, H., Lv, C., Fu, X., and Nie, J. 2009. Review of Practical Experience of Polymer Flooding at Daqing. *SPE Res Eval & Eng* **12** (3): 470–476. SPE-114342-PA. doi: 10.2118/114342-PA.

Wang, D.M., Seright, R.S., Shao, Z., and Wang, J. 2008. Key Aspects of Project Design for Polymer Flooding at the Daqing Oil Field. *SPE Res Eval & Eng* **11** (6): 1117–1124. SPE-109682-PA. doi: 10.2118/109682-PA.

Wreath, D., Pope, G.A., and Sepehrnoori, K. 1990. Dependence of Polymer Apparent Viscosity on the Permeable Media and Flow Conditions. *In Situ* **14** (3): 263–283.

Zaitoun, A. and Kohler, N. 1987. The Role of Adsorption in Polymer Propagation Through Reservoir Rocks. Paper SPE 16274 presented at the SPE International Symposium on Oilfield Chemistry, San Antonio, Texas, USA, 4–6 October. doi: 10.2118/16274-MS.

Zhang, G. and Seright, R.S. 2007. Conformance and Mobility Control: Foams vs. Polymers. Paper SPE 105907 presented at the International Symposium on Oilfield Chemistry, Houston, 28 February–2 March. doi: 10.2118/105907-MS.

SI Metric Conversion Factors

cp $\times$ 1.0*	E$-$03 = Pa·s
ft $\times$ 3.048*	E$-$01 = m
in. $\times$ 2.54*	E+00 = cm
md $\times$ 9.869 233	E$-$04 = μm^2
psi $\times$ 6.894 757	E+00 = kPa

*Conversion factor is exact.

Randy Seright is a senior engineer at the New Mexico Petroleum Recovery Research Center at New Mexico Tech in Socorro, New Mexico, where he has worked since 1987. email: randy@prrc.nmt.edu. He holds a PhD degree in chemical engineering from the University of Wisconsin at Madison. Seright received the SPE/DOE IOR Pioneer Award in 2008. **Tianguang Fan** is a research chemist at the New Mexico Petroleum Recovery Research Center. email: tfan@nmt.edu. **Kate Wavrik** is a laboratory associate at the New Mexico Petroleum Recovery Research Center. email: kate@prrc.nmt.edu. **Rosangela de Carvalho Balaban** is a professor of chemistry at the Universidade Federal do Rio Grande do Norte in Natal, Brazil. email: balaban@supercabo.com.br.